applied sciences

MDPI

Article

Optimizing Paste and Mortar Margins (α and β) to Enhance Compressive Strength in Cemented Sand, Gravel and Rock

Wambley Adomako Baah [1,*], Jinsheng Jia [1], Cuiying Zheng [1], Yue Wang [1,2], Baozhen Jia [1,2] and Yangfeng Wu [2,3]

[1] State Key Laboratory of Simulation and Regulation of Water Cycle in River Basin, China Institute of Water Resources and Hydropower Research (IWHR), Beijing 100038, China; jiajsh@iwhr.com (J.J.); zhengcy@iwhr.com (C.Z.); yue.wang@bjtu.edu.cn (Y.W.); jiabaozhen1987@sohu.com (B.J.)
[2] School of Civil Engineering, Beijing Jiaotong University, Beijing 100044, China; wuyangfeng_0211@tju.edu.cn
[3] State Key Laboratory of Hydraulic Engineering Simulation and Safety, Tianjin University, Tianjin 300072, China
* Correspondence: wambleybaah@gmail.com

Abstract: A suitable range of paste and mortar margins (α and β) to enhance compressive strength in Rich-Mix cemented sand gravel and rock (CSGR) material for application in CSGRD construction is critical. SL 678-2014 recommends margins > 1, which are specifically designed to fill the voids within the fine and coarse aggregates with paste and mortar, respectively, while allowing some excess for workability. However, the optimum ranges of values after 1 are inadequately determined, often leading to high efforts and time-consuming trial mixes that are not economical. This study evaluates two datasets to identify the optimal ranges of α and β margins for compressive strength development in Rich-Mix CSGR, aiming to achieve the compressive strength class $C_{180}20$, intended for use as cushion, protective, and seepage control layers in CSGRD. Using Pearson correlations, t-statistics, and *p*-values, the first dataset (7, 28, 90, and 180 days) showed weak correlations between paste margins and compressive strengths (coefficients 0.172 to 0.418, *p*-values > 0.05) and negligible relationships for mortar margins (coefficients −0.269 to 0.204, *p*-values > 0.05), affirming the contribution of other factors in the compressive strength development in CSGR. The second dataset (14, 28, 90, and 180 days) revealed significant positive correlations between paste margins and strengths at 14, 90, and 180 days (coefficients up to 0.850, *p*-values < 0.05). Mortar margins, however, negatively impacted strength (coefficients −0.544 to −0.628, *p*-values < 0.05), revealing the need to control the sand ratio. The optimal range of values was $1.05 \leq \alpha \leq 1.09$ and $1.15 \leq \beta \leq 1.25$, with a water–binder ratio of 0.7~1.3, vibrating–compacted value (VC) of 2~8 s, and sand ratio of 18~35%. These findings highlight the significance of precise paste and mortar margin ranges in the compressive strength development of Rich-Mix CSGR.

Keywords: cemented sand; gravel and rock dam; Rich-Mix CSGR; paste margin (α); mortar margin (β); compressive strength development; $C_{180}20$; Pearson correlation coefficient

Citation: Baah, W.A.; Jia, J.; Zheng, C.; Wang, Y.; Jia, B.; Wu, Y. Optimizing Paste and Mortar Margins (α and β) to Enhance Compressive Strength in Cemented Sand, Gravel, and Rock. *Appl. Sci.* **2024**, *14*, 10881. https://doi.org/10.3390/app142310881

Academic Editor: Tiago Miranda

Received: 8 September 2024
Revised: 24 October 2024
Accepted: 22 November 2024
Published: 24 November 2024

1. Introduction

Cemented Sand Gravel and Rock Dam (CSGRD) is a new environmentally friendly type of dam with characteristics between those of an embankment (soil–rock) dam and a concrete dam developed and promoted by Professor Jinsheng Jia of China, the Honorary President of the International Committee on Large Dams (ICOLD) [1–4]. It addresses the challenges of breaching in embankment dams due to overtopping and erosion, as well as the high environmental and economic costs of concrete gravity dam construction due to high cement consumption and foundation requirements [5,6].

Based on the concepts of Hardfill [7] and Cemented Sand and Gravel (CSG) Dams [8–10], CSGRD further expanded the use of local aggregate [11] sizes from 80 mm to 150

mm and 300 mm for dam and cofferdam construction, respectively. The dam can be built with locally available materials with little or no screening [12]. The materials are cemented with cementitious materials to produce Cemented Sand Gravel and Rock (CSGR) of certain shear strength, as specified by the Technical Guideline for Cemented Materials Dam (SL678-2014) [13–15].

CSGRD, like a Roller Compacted Concrete (RCC) dam, Hardfill Dam, or Cemented Sand and Gravel (CSG) Dam, has seepage lines along its compacted layers and requires protective watertight layers. It also requires cushion layers for the dam body. Therefore, Jia et al. (2016) recommended that if the Rich-Mix CSGR can attain a frost resistance grade of F300 (attain mass loss of less than 5% or maintain 60% of its initial dynamic modulus after 300 freeze and thaw cycles) and a permeability resistance grade of W12 (i.e., equivalent to a permeability coefficient of 0.13×10^{-10} m/s), it can be used to achieve frost resistance, to construct protective and seepage control layers and cushions, and also applied in anti-carbonation zones in CSGRD. This criterion, however, is flexible depending on the project requirements [1].

Though SL678-2014 specifies the paste margin (α) > 1 and mortar margin (β) > 1, for the Rich-Mix CSGR material, the actual values achieved via experimentation are usually lower or more than required due to the complexity of the experiment, as well as being labor and time-intensive, resulting in an inadequately studied correlation behaviour [14]. The α value represents the paste volume-to-fine aggregate void ratio, while the β value represents the mortar volume-to-coarse aggregate void ratio [14]. The sizes of the α and β values reflect the thickness of the excess or wrapping layer of paste and mortar for fine and coarse aggregates, respectively. When α and β values exceed 1, additional paste and mortar are available for workability margin. The minimum values of α and β must not fall below 1 to ensure sufficient cohesion and prevent significant mixture segregation during transport, spreading, and compaction. Using this technique to ensure optimum paste and mortar margins in mix proportioning ensures optimum paste and mortar volumes required for the project other than guesswork or a series of trial proportioning methods that waste resources [14].

Again, research has stated that the primary characteristic of cemented sand, gravel, and rock is that, the aggregate used is unscreened, leading to a discrete and fluctuating gradation. To address this challenge, they indicated that, an optimized mix proportion design method can be achieved by adjusting the sand content or sand ratio and optimizing the aggregate gradation as well to control the workability margins [15,16].

Furthermore, to achieve the desirable workable margin, the cementitious materials-to-mortar ratio of High-Cementitious Paste Roller Compacted Concrete (HCRCC) , according to the United States Army Corps of Engineers (USACE), needs to lie in the range of 0.34 to 0.40 [16]. According to the United States Bureau of Reclamation (USBR), a paste-to-mortar ratio of not less than 42% can yield a design compressive strength and direct tensile strength of 11 to 40 MPa and 0.7 to 2.9 MPa, respectively [16,17].

USACE also studied the relationship between the α and β values for 12 mixes of (Super-High-Cementitious Roller Compacted Concrete (SHCRCC) to achieve optimized workability. The α values ranged from 1.5 to 1.9, while the β values ranged from 1.8 to 2.2. When cementitious materials were partially replaced with Stone Powder (SP), the α value decreased while the β value increased. It was concluded that this condition typically occurs because the proportion of fine aggregates rises and the proportion of coarse aggregates falls as the SP volume increases. As the fine aggregate content increases, the paste volume decreases, leading to a gradual reduction in workability and strength [17].

Beyond basic strength, a modern Roller Compacted Concrete (RCC) mix is defined by its paste-to-mortar (p/m) and sand-to-aggregate (s/a) ratios, Maximum Size of Aggregate (MSA), and modified Vee-Bee time. These factors influence the density, compaction ratio, and material segregation tendency. During construction, these properties determine workability and whether the RCC is permeable with weak planes or cohesive, seamless, watertight, and dense [18].

Interestingly, researchers tend to adopt mineral admixtures in low-cement mixtures to increase paste volume for filling aggregate voids and coating particles to achieve optimized paste and mortar margins. However, in mixtures with unprocessed aggregates containing clay and friable particles, these admixtures may not improve long-term strength, especially when high water-to-cement (w/c) ratios are used; therefore, sand containing deleterious fine content (natural particles < 80 μm) of more than 20% needs to be avoided [19,20].

To achieve a density of 98.5% in the overall approach of RCC (where the dam body is designed to withstand seepage), as opposed to the separate approach [7] (where a separate layer is designed upstream to manage seepage), a paste-to-mortar ratio of 0.37 needs to be considered. To minimize segregation from the usage of larger aggregates, it is suitable to consider a Maximum Size of Aggregate (MSA) of 37.5 to 40 mm. Additionally, the percentage of aggregate passing the 40 mm sieve should be 80% to 90% [18].

In a cementitious mix with a single-sized aggregate (as shown in Figure 1a), more cementitious paste is needed to fill gaps between fine aggregates and mortar to fill gaps in coarse aggregates to eliminate excess air voids. Using multi-sized aggregate (as shown in Figure 1b,c) reduces the gap volume, lowering the paste and mortar requirement. If the paste and mortar volumes remain constant with multi-sized aggregate, the excess paste and mortar increase, improving workability by coating the particles [21]. Therefore, aggregate grading significantly affects paste and mortar demand and cementitious mix workability, as indicated in Figure 1.

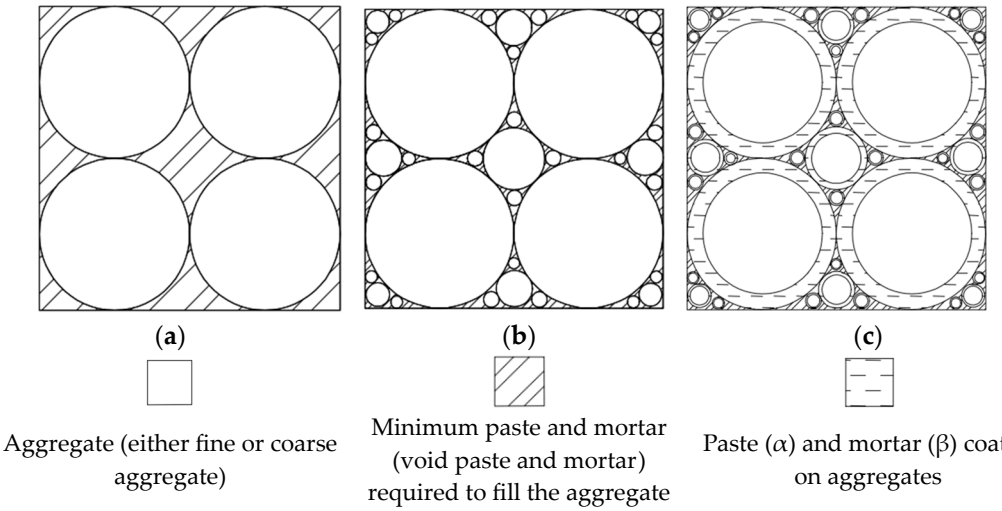

Figure 1. (**a**) Cementitious mix with single-sized aggregate. (**b**) Reduction in cement paste or mortar volume due to a smaller volume of gaps within the aggregate skeleton. (**c**) Improving workability at the same paste or mortar volume due to the formation of paste or mortar coating on aggregate surfaces.

Mohammed et al. (2012) indicated during the study of the optimization of conventional concrete by minimizing void volume in the aggregate mixture system that the results emphasized the need for sufficient filler material and cement paste for larger particles to ensure effective binding. Slightly overfilling aggregate voids improves concrete workability and fluidity during casting. Replacing crushed material with sand enhances workability and reduces voids due to the easy slip of smooth, rounded grains. Additionally, slump tests indicated that concretes with optimal aggregate distribution and minimal voids require only a small amount of cementitious paste to achieve the high strength of the material [22].

Compared to Conventional Vibrated Concrete (CVC), a lower sand-to-aggregate ratio of less than 0.35 was optimal for achieving consistency in the RCC mix. For lean RCC,

medium paste, and high paste RCC, the Vee-Bee time of not more than 30 s, 10–20 s, and 8–15 s, respectively, were found to achieve optimum workability [18].

In studying the permeable character of Cemented Sand and Gravel (CSG) Dams and their seepage fields, Zhao et al. (2018) indicated that the mortar margin and cementation strength of well-graded partial CSG material tend to be superior, whereas those of poorly graded CSG materials appear to be weaker [23].

For optimal density in CSGR through vibration and consolidation, sand voids should be filled with paste, and voids within the gravel and rock should be filled with mortar, forming a highly solidified and dense structure. As the α or β values increase to the optimal or limit values, the VC value decreases accordingly, enhancing workability, strength, and durability. Conversely, if the α and β values fall below the limit, excess air fills the voids, leading to serious segregation, durability issues, and strength reduction. The α value depends on the paste content and the void content of the fine aggregate, while the β value depends on the mortar content and the voids within the coarse aggregates. The equations for paste and mortar margin used in optimizing the mix in this study are provided in Equations (A1)–(A5) in Appendix A.

In conclusion, the paste and mortar margins are crucial parameters yet understudied in the field of CSGRD; therefore, this research paper seeks to answer the duo questions: What is the optimum range of paste and mortar margins, and how is the behaviour of the relationship between paste and mortar margins with the compressive strength development of the Rich-Mix CSGR towards the achievement of $C_{180}20$ for cushion, protective, and seepage control layers in CSGRD construction? This research considers two case study projects, with details provided in Appendix A. The answers to the questions will help to understand the relationship between the paste and mortar margins and compressive strength development in CSGR and other similar materials, aiding in the optimization of material mixes for the construction of more resilient, economic, and sustainable hydraulic structures in the future, benefiting the entire dam industry enormously.

2. Materials and Methods

2.1. Materials (Lengshuihe Auxiliary CSGRD)

2.1.1. Cementitious Materials

The test used a grade 42.5 ordinary Portland cement produced by Sichuan Esheng Cement Group Co., Ltd. (Leshan, China). The cement quality and chemical test results are listed in Tables 1 and 2, respectively, and the cement mortar strength test results are shown in Table 3. It can be seen from both tables that the test results of the inspected properties meet the technical requirements specified in GB175-2020 [24] "General Portland Cement" (ASTM C150 equivalent) [25]. The test used Class II fly ash produced by the Pannan Power Plant of Guizhou Yueqian Electric Power Co., Ltd. (Liupanshui, China) owned by Power Construction Corporation of China. The test results of the performance and the chemical analysis of the fly ash are shown in Tables 4 and 5. The tables show that the test results of the tested performance comply with GB/T1596-2017 [26] Class II fly ash coal ash requirements (ASTM C618 equivalent) [27].

Table 1. Cement quality test results.

Item	Density (g/cm ^{3})	Fineness (%)	Specific Surface Area (cm^2/g)	Standard Consistency (%)	Setting Time (min)		Stability
					Initial Setting	Final Setting	
Cement	3.16	6.6	3610	27.2	140	190	qualified
GB175-2023 requirements	-	-	-	-	≥45	≤600	qualified

Table 2. Chemical analysis of cement.

Component	CaO	SiO_2	Al_2O_3	Fe_2O_3	MgO	SO_3	Na_2O	K_2O	LOI
Percentage (%)	60–67	17–25	3–8	0.5–6	0.5–4	1–3	0.1–1	0.1–1	0.5–3

Table 3. Cement mortar strength test results.

Item	Flexural Strength (MPa)		Compressive Strength (MPa)	
	3d	28d	3d	28d
Cement	5.7	7.8	30.6	49.5
GB175-2023 requirements	≥3.5	≥6.5	≥17.0	≥42.5

Table 4. Fly ash performance test results.

Item	Density (g/cm ^{3})	Fineness (%)	Water Demand Ratio (%)	Activity Index (%)
Fly ash	2.47	20.0	98	70.6
GB/T1596-2017 Level II requirements	-	≤30	≤105	≥70

Table 5. Chemical analysis of fly ash.

Component	SiO_2	Al_2O_3	Fe_2O_3	CaO	MgO	SO_3	Na_2O	K_2O	LOI
Percentage (%)	40–60	15–35	5–15	5–30	1–5	0.5–4	0.5–1.5	0.5–1.5	1–5

2.1.2. Aggregates

The aggregate properties [28] of the excavated reservoir materials used in the production of the CSGR for the body of the dam during the construction are provided in Tables 6–8. According to the "Hydraulic Concrete Test Regulations" SL/T 352-2020 [29], the apparent density and water absorption of the fine and coarse aggregate were tested (based on the saturated surface dry state). The results are shown in Tables 6 and 7 for both the coarse and fine aggregates, respectively. As can be seen from Table 6, the apparent density of coarse aggregate is between 2590 kg/m^3~2790 kg/m^3, and the saturated surface dry water absorption rate is between 0.22%~6.14%. The gradation envelope for the mix proportioning design is provided in Figure A3 Appendix A.

Table 6. Coarse aggregate test results.

Aggregate	Apparent Density (kg/m^3)				Water Absorption Rate (%)			
	80~150 mm	40~80 mm	20~40 mm	5~20 mm	80~150 mm	40~80 mm	20~40 mm	5~20 mm
Gravel and rock	2790	2850	2760	590	0.23	0.77	3.06	6.14

Table 7. Fine aggregate test results.

Aggregate type	Fineness modulus	Mud content (%)	Apparent Density (kg/m^3)	Water Absorption Rate (%)
river sand	2.89	<1	2348	8.95

Table 8. Proportions of particle size distribution in sampled aggregates.

Grading No.	Proportion of Coarse Aggregate (%)				
	0~5 mm	5~20 mm	20~40 mm	40~80 mm	80~150 mm
A1	19.4	21.3	23.9	27.3	8.1
A2	8.3	35.9	31.6	20.7	3.5
A3	12.1	25.9	29.7	27.5	4.7

A4	13.0	27.2	33.2	23.4	3.2

2.2. Materials (Shaping I Hydropower CSGRD)

2.2.1. Cementitious Materials

The test used grade 42.5 ordinary Portland cement produced by Sichuan Esheng Cement Group Co., Ltd. The cement quality and chemical test results are listed in Tables 9 and 10, respectively, and the cement mortar strength test results are shown in Table 11. It can be seen from the table that the test results of the inspected properties meet the technical requirements specified in GB175-2020 [24]"General Portland Cement" (ASTM C150 equivalent)[25]. The test used Class II fly ash produced by the Pannan Power Plant of Guizhou Yueqian Electric Power Co., Ltd (Liupanshui, China) owned by Power Construction Corporation of China. The test results of the fly ash, including the performance and the chemical analysis, are shown in Tables 12 and 13. From the tables, it can be seen that the test results of the tested performance comply with GB/T1596-2017 [26] Class II fly ash. coal ash requirements (ASTM C618 equivalent)[27].

Table 9. Cement quality test results.

Item	Density (g/cm ^{3})	Fineness (%)	Specific Surface Area (cm^2/g)	Standard Consistency (%)	Setting Time (min)		Stability
					Initial Setting	Final Setting	
Cement	3.16	6.6	3610	27.2	140	190	qualified
GB175-2023 requirements	-	-	-	-	≥45	≤600	qualified

Table 10. Chemical analysis of cement.

Component	CaO	SiO_2	Al_2O_3	Fe_2O_3	MgO	SO_3	Na_2O	K_2O	LOI
Percentage (%)	60–67	17–25	3–8	0.5–6	0.5–4	1–3	0.1–1	0.1–1	0.5–3

Table 11. Cement mortar strength test results.

Item	Flexural Strength (MPa)		Compressive Strength (MPa)	
	3d	28d	3d	28d
Cement	5.7	7.8	30.6	49.5
GB175-2023 requirements	≥3.5	≥6.5	≥17.0	≥42.5

Table 12. Fly ash performance test results.

Item	Density (g/cm^3)	Fineness (%)	Water Demand Ratio (%)	Activity Index (%)
Fly ash	2.47	20.0	98	70.6
GB/T1596-2017 Level II requirements	-	≤30	≤105	≥70

Table 13. Chemical analysis of fly ash.

Component	SiO_2	Al_2O_3	Fe_2O_3	CaO	MgO	SO_3	Na_2O	K_2O	LOI
Percentage (%)	40–60	15–35	5–15	5–30	1–5	0.5–4	0.5–1.5	0.5–1.5	1–5

2.2.2. Aggregates

The aggregate properties [28] of the excavated reservoir materials used in the production of the CSGR for dam construction are provided in Tables 14–16. According to the "Hydraulic Concrete Test Regulations" SL/T 352-2020 [29], the apparent density and water

absorption of the fine and coarse aggregate were tested (based on the saturated surface dry state). The results are shown in Tables 10 and 11 for both the coarse and fine aggregates, respectively. As can be seen from Table 10, the apparent density of coarse aggregate is between 2720 kg/m^3~2762 kg/m^3, and the saturated surface dry water absorption rate is between 0.22%~0.81%. The gradation envelope for the mix proportioning design is provided in Figure A5 in the Appendix A.

Table 14. Coarse aggregate test results.

Aggregate	Apparent Density (kg/m^3)				Water Absorption Rate (%)			
	80~150 mm	40~80 mm	20~40 mm	5~20 mm	80~150 mm	40~80 mm	20~40 mm	5~20 mm
Gravel and rock	2722	2720	2750	2762	0.22	0.48	0.50	0.81

Table 15. Fine aggregate test results.

Aggregate Type	Fineness Modulus	Mud Content (%)	Apparent Density (kg/m^3)	Water Absorption Rate (%)
river sand	2.86	<1	2690	1.5

Table 16. Proportions of particle size distribution in sampled aggregates.

Grading No.	Sand Rate	Proportion of Coarse Aggregate (%)			
		5~20 mm	20~40 mm	40~80 mm	80~150 mm
B1	18	7.00	28.00	13.00	52.00
B2	35	39.00	26.00	21.00	14.00
B3	26.50	21.15	27.12	16.54	35.20

3. Methods

3.1. Mix Proportioning, Sample Preparation, and Testing

First, aggregates of the average gradation (as shown from the gradation envelope in Figures A4 and A5) were divided into five classes based on their diameters (using sieve analysis): fine aggregate (0–5 mm), small stones (5–20 mm), medium stones (20–40 mm), large stones (40–80 mm), and extra-large stones (80–150 mm) [25]. Secondly, aggregates from each class were measured according to the determined trial mix proportioned by weight and mixed in a batch mixer with water, cement [24,25], fly ash [26,27], and water reducer in their appropriate proportions as indicated in Tables 17 and 18. Afterwards, the fresh mix was wet-screened to remove aggregates greater than 40 mm in diameter, as required by SL 678-2014[14]. The vibrating–compacted (VC) value, which measures the workability of the mixture, was determined using the Vebe apparatus [30], shown in Figure A6 in the appendix. Compressive test samples were prepared from the wet-sieved mix in the laboratory according to SL 678-2014 [14] and ASTM C39/C39M [31] guidelines. Molded samples were cured in a steam curing chamber at a temperature of 20 °C and a relative humidity of 95% until each test age according to ASTM C192/192M [32]. At each test age, three specimens (1 sample) were tested by crushing using the compressive strength test machine as indicated in Figure 2, and the average value was recorded. The experiment was conducted for various sand ratios (18% to 35%) and different cementitious contents to study the development of compressive strength with curing age in each project according to SL 678-2014 [14] guidelines.

Table 17. Series of laboratory mixes for compressive strength development (Lengshuihe Auxiliary CSGRD).

Material Usage (kg/m^3)	Compressive STRENGTH

Serial No.	Cement	Fly Ash	Water	Gravel and Rocks	Water–Binder Ratio	Water Reducer (%)	VC Value (s)	Sand Rate (%)	7d	28d	90d	180d
1	50	50	80	2395	0.8	1	2.4		1.1	1.3	2.0	2.0
2	60	60	84	2428	0.7	1	6.5	25	1.6	1.9	2.7	2.8
3	70	70	91	2460	0.7	1	7.8		1.9	2.3	3.7	3.8
4	50	50	70	2386	0.7	1	6.7		1.0	1.4	2.0	2.1
5	60	60	84	2419	0.7	1	6.9		1.5	2.1	3.0	3.2
6	70	70	98	2451	0.7	1	6.5	30	1.7	2.5	3.8	3.9
7	80	80	112	2368	0.7	1	7.0		1.7	2.6	4.1	4.4
8	100	100	140	2400	0.7	1	6.8		2.3	3.8	6.0	6.3
9	50	50	70	2432	0.7	1	6.6		1.8	2.2	3.5	4.0
10	60	60	84	2349	0.7	1	6.8		1.7	2.4	3.9	4.1
11	70	70	98	238 6	0.7	1	6.9	35	1.9	2.7	3.9	4.4
12	70	70	98	242 8	0.7	1	7.6		3.1	5.7	6.6	—
13	70	70	98	2330	0.7	1	7.5		5.8	10.7	13.2	—
14	70	70	98	2363	0.7	1	7.9		8.3	14.7	16.0	—
15	50	50	70	2395	0.7	1	3.8		5.9	8.5	—	—
16	60	60	84	2321	0.7	1	3.9	25	7.5	9.5	—	—
17	70	70	98	2354	0.7	1	3.6		8.5	11.4	—	—
18	50	50	70	2386	0.7	1	4.9		5.2	6.8	—	—
19	60	60	84	2395	0.7	1	4.5	30	7.4	9.9	—	—
20	70	70	98	2428	0.7	1	4.7		8.1	11.9	—	—

Table 18. Series of laboratory mixes for compressive strength development (Shaping I Hydropower CSGRD).

Serial No.	Material usage (kg/m³)								Compressive Strength			
	Cement	Fly Ash	Water	Gravel and Rocks	Water–Binder Ratio	Water Reducer (%)	VC Value (s)	Sand Rate (%)	14d	28d	90d	180d
1	35	35	87	2395	1.24	1	5.0	35.0	1.8	3.1	3.9	5.6
2	35	35	75	2428	1.07	1	5.0	26.5	2.6	3.3	4.8	6.0
3	35	35	63	2460	0.9	1	2.0	18	5.2	8.9	10.8	16.2
4	40	40	87	2386	1.09	1	5.0	35.0	2.6	3.5	3.9	6.4
5	40	40	75	2419	0.94	1	3.5	26.5	2.9	5.0	6.5	9.1
6	40	40	63	2451	0.79	1	0.5	18	5.7	8.2	12	14.9
7	50	50	87	2368	0.87	1	5.0	35.0	2.7	5.1	7.1	9.3
8	50	50	75	2400	0.75	1	3.0	26.5	4.5	5.4	9.4	9.8
10	50	50	63	2432	0.63	1	0.5	18	6.5	11.2	15.2	20.4
11	60	60	87	2349	0.73	1	4.5	35.0	3.9	5.7	9.4	10.4
12	60	60	75	238 6	0.63	1	2.0	26.5	7.6	9.9	12.2	18.0
13	60	60	60	242 8	0.5	1	0.5	18	10.7	15.8	21.4	28.8
14	70	70	87	2330	0.62	1	5.0	35.0	6.2	8.6	11.9	15.7
15	70	70	75	2363	0.54	1	2.5	26.5	7.3	11.0	16	20.0
16	70	70	63	2395	0.45	1	0.5	18	11.7	15.5	25.7	28.2
17	75	75	87	2321	0.58	1	3.5	35.0	7.3	7.9	15.8	14.4
18	75	75	75	2354	0.5	1	2.0	26.5	10.0	14.6	20.3	26.6

(**a**) (**b**)

Figure 2. (**a**) Laboratory compressive strength test sample preparation. (**b**) Testing.

3.2. Steps for the Determination of the Paste and Mortar Margins

The Equations (from 1 to 5) discussed in Appendix A were used to determine the paste and mortar margins after the material properties required by these Equations were established. This was accomplished through a series of compressive strength trial experiments using different sand ratios, binder-to-water ratio methods, and guidelines as specified in SL678-2014 [14], ASTM C39/C39M [31], and SL/T 352 [29].

3.3. Steps to Use Pearson Correlation and Assess Statistical Significance

Pearson Correlation is a parametric statistical method used to measure the strength and direction of the relationship between two variables [33,34]. It produces a score from −1 to +1, where values closer to ±1 indicate a strong correlation and values near zero indicate no correlation. This method is most effective for normally distributed data [33,34].

Five steps were considered for the application of the Pearson correlation and the determination of the statistical significance in this work. The detailed steps of sample calculation are provided in Appendix A [33,34].

4. Results and Discussion

4.1. Results

4.1.1. Workability (VC Value), Paste Margin (α), Mortar Margin (β), Pearson Correlation Coefficient, and Compressive Strength Development

Tables 19 and 20 show the results of the workability (using the Vebe test) of the freshly prepared CSGR mixture after wet-sieving, the paste and mortar margins calculated from Equations (A1)–(A5) in Appendix A, and the results of a series of tests on the averages of the compressive strength development for both projects at 7 days, 14 days, 28 days, 90 days, and 180 days. Table 21 shows the completed Pearson correlation and statistical significance (t-statistics and *p*-values) between the paste and mortar margins and the compressive strength development for both projects under study.

Table 19. Lengshuihe Auxiliary CSGRD.

Serial No.	Material Usage (kg/m³)				Water–Binder Ratio	Water Reducer (%)	VC Value (s)	α	β	Sand Rate (%)	Compressive Strength			
	Cement	Fly Ash	Water	Gravel and Rocks							7d	28d	90d	180d
1	50	50	80	2395	0.8	1	2.4	0.057	0.179		1.1	1.3	2.0	2.0
2	60	60	84	2428	0.7	1	6.5	0.058	0.172	25	1.6	1.9	2.7	2.8
3	70	70	91	2460	0.7	1	7.8	0.062	0.166		1.9	2.3	3.7	3.8

4	50	50	70	2386	0.7	1	6.7	0.040	0.227		1.0	1.4	2.0	2.1
5	60	60	84	2419	0.7	1	6.9	0.048	0.221		1.5	2.1	3.0	3.2
6	70	70	98	2451	0.7	1	6.5	0.056	0.215	30	1.7	2.5	3.8	3.9
7	80	80	112	2368	0.7	1	7.0	0.064	0.209		1.7	2.6	4.1	4.4
8	100	100	140	2400	0.7	1	6.8	0.080	0.197		2.3	3.8	6.0	6.3
9	50	50	70	2432	0.7	1	6.6	0.030	0.276		1.8	2.2	3.5	4.0
10	60	60	84	2349	0.7	1	6.8	0.037	0.270		1.7	2.4	3.9	4.1
11	70	70	98	238 6	0.7	1	6.9	0.044	0.264	35	1.9	2.7	3.9	4.4
12	70	70	98	242 8	0.7	1	7.6	0.056	0.215		3.1	5.7	6.6	—
13	70	70	98	2330	0.7	1	7.5	0.056	0.215		5.8	10.7	13.2	—
14	70	70	98	2363	0.7	1	7.9	0.056	0.215		8.3	14.7	16.0	—
15	50	50	70	2395	0.7	1	3.8	0.049	0.178		5.9	8.5	—	—
16	60	60	84	2321	0.7	1	3.9	0.058	0.172	25	7.5	9.5	—	—
17	70	70	98	2354	0.7	1	3.6	0.067	0.166		8.5	11.4	—	—
18	50	50	70	2386	0.7	1	4.9	0.040	0.227		5.2	6.8	—	—
19	60	60	84	2395	0.7	1	4.5	0.048	0.221	30	7.4	9.9	—	—
20	70	70	98	2428	0.7	1	4.7	0.056	0.215		8.1	11.9	—	—

Table 20. Shaping I Hydropower CSGRD.

	Material Usage (kg/m³)										**Compressive Strength**			
Serial No.	**Cement**	**Fly Ash**	**Water**	**Gravel and Rocks**	**Water–Binder Ratio**	**Water Reducer (%)**	**VC Value (s)**	**α**	**β**	**Sand Rate (%)**	**14d**	**28d**	**90d**	**180d**
1	35	35	87	2395	1.24	1	5.0	0.068	0.337	35.0	1.8	3.1	3.9	5.6
2	35	35	75	2428	1.07	1	5.0	0.072	0.242	26.5	2.6	3.3	4.8	6.0
3	35	35	63	2460	0.9	1	2.0	0.070	0.167	18	5.2	8.9	10.8	16.2
4	40	40	87	2386	1.09	1	5.0	0.071	0.337	35.0	2.6	3.5	3.9	6.4
5	40	40	75	2419	0.94	1	3.5	0.073	0.252	26.5	2.9	5.0	6.5	9.1
6	40	40	63	2451	0.79	1	0.5	0.073	0.167	18	5.7	8.2	12	14.9
7	50	50	87	2368	0.87	1	5.0	0.076	0.337	35.0	2.7	5.1	7.1	9.3
8	50	50	75	2400	0.75	1	3.0	0.079	0.252	26.5	4.5	5.4	9.4	9.8
10	50	50	63	2432	0.63	1	0.5	0.079	0.117	18	6.5	11.2	15.2	20.4
11	60	60	87	2349	0.73	1	4.5	0.081	0.337	35.0	3.9	5.7	9.4	10.4
12	60	60	75	238 6	0.63	1	2.0	0.084	0.252	26.5	7.6	9.9	12.2	18.0
13	60	60	60	242 8	0.5	1	0.5	0.083	0.167	18	10.7	15.8	21.4	28.8
14	70	70	87	2330	0.62	1	5.0	0.086	0.337	35.0	6.2	8.6	11.9	15.7
15	70	70	75	2363	0.54	1	2.5	0.090	0.252	26.5	7.3	11.0	16	20.0
16	70	70	63	2395	0.45	1	0.5	0.092	0.167	18	11.7	15.5	25.7	28.2
17	75	75	87	2321	0.58	1	3.5	0.088	0.337	35.0	7.3	7.9	15.8	14.4
18	75	75	75	2354	0.5	1	2.0	0.092	0.252	26.5	10.0	14.6	20.3	26.6

Table 21. Completed Pearson correlation coefficients and statistical significance of both CSGRD study cases.

	Lengshuihe Auxiliary CSGRD				**Shaping I Hydropower CSGRD**			
Margins	**Test Age (days)**	**Pearson Correlation (r)**	**t-Statistics**	***p*-Value**	**Test Age (days)**	**Pearson Correlation (r)**	**t-Statistics**	***p*-Value**
Paste Margin (α)	07	0.172	0.741	4.67×10^{-1}	14	0.844	6.785	1.07×10^{-5}
	28	0.197	0.853	4.04×10^{-1}	28	0.787	5.252	1.06×10^{-4}
	90	0.221	0.784	4.43×10^{-1}	90	0.850	6.986	7.96×10^{-6}

	180	0.418	1.382	1.84×10^{-1}	180	0.787	5.252	1.06×10^{-4}
Mortar Margin (β)	07	−0.269	−1.185	2.51×10^{-1}	14	−0.544	2.568	1.96×10^{-2}
	28	−0.216	−0.936	3.62×10^{-1}	28	−0.628	3.222	5.3×10^{-3}
	90	−0.003	−0.011	9.91×10^{-1}	90	−0.565	2.748	1.46×10^{-2}
	180	0.204	0.624	5.40×10^{-1}	180	−0.628	3.222	5.30×10^{-3}

4.1.2. Graphical Representation of the Behavior of the Relationship Between Paste Margins, Mortar Margins, and Compressive Strength Development

Figures 3 and 4 provide a graphical representation of the behaviour of the relationship or correlation between the paste margin, mortar margin, and the compressive strength development of all curing days of the CSGR material or samples for both the Lengshuihe CSGRD and Shaping I CSGRD, respectively. These graphs offer a straightforward way to select the appropriate margins or paste-to-mortar ratio for the $C_{180}20$ or lower compressive design strength of Rich-Mix CSGR for CSGRD applications during the compressive strength trial tests in the laboratory. Once the paste and mortar margins are selected from the chart based on the compressive strength required and the sand ratio is also known (18–35%) [14] as well as the coarse aggregate content, the void content in the fine aggregate and coarse aggregate is then determined per cubic meter using packing density or any acceptable method. The paste and mortar can then be computed with the help of Equations (A1)–(A5) in Appendix A. This saves time, money, and energy while boosting technician confidence. Note that the value on the chart is the excess paste and mortar; the user needs to add 1 (i.e., void paste or mortar = 1) to each value to have the total paste or mortar margin as shown in the conclusion. Depending on the strength requirement for the Rich-Mix CSGR, the 180-day graphs in either project may be used for the selection of paste and mortar margins where applicable. The properties of the materials to be used in any project of CSGR can be compared to those of the materials discussed in Section 2 of this paper in conjunction with SL678-2014 [14], the technical guideline for cemented granular materials.

(1) Project 1: Lengshuihe Auxiliary CSGRD

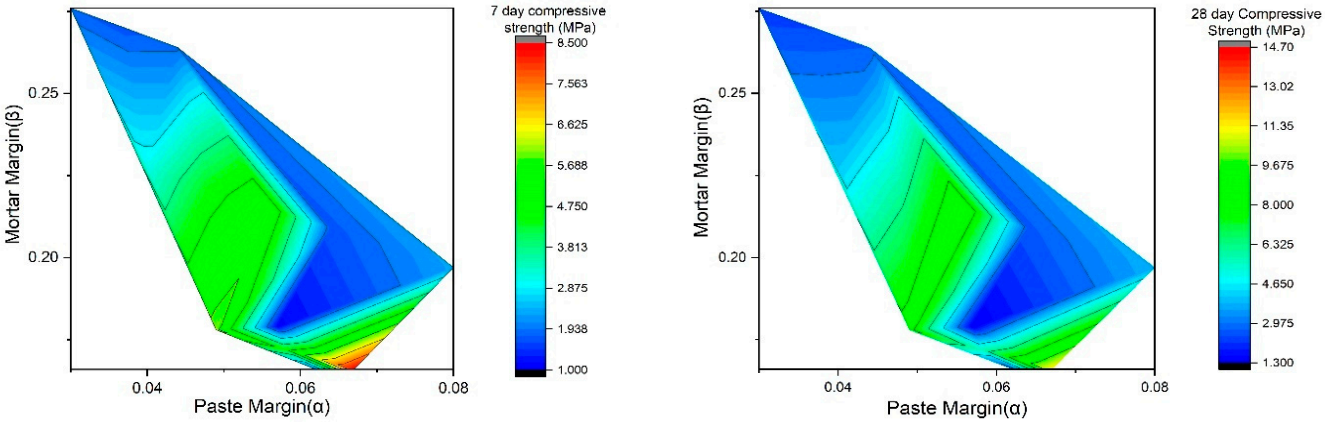

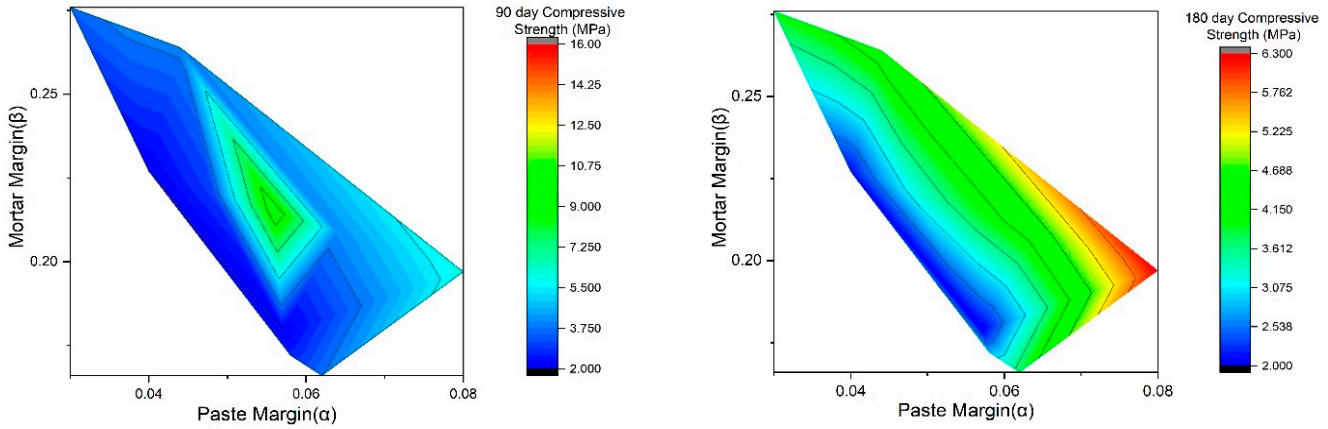

Figure 3. Relationship between paste and mortar margins and compressive strength development.

(2) Project 2: Shaping I Hydropower CSGRD

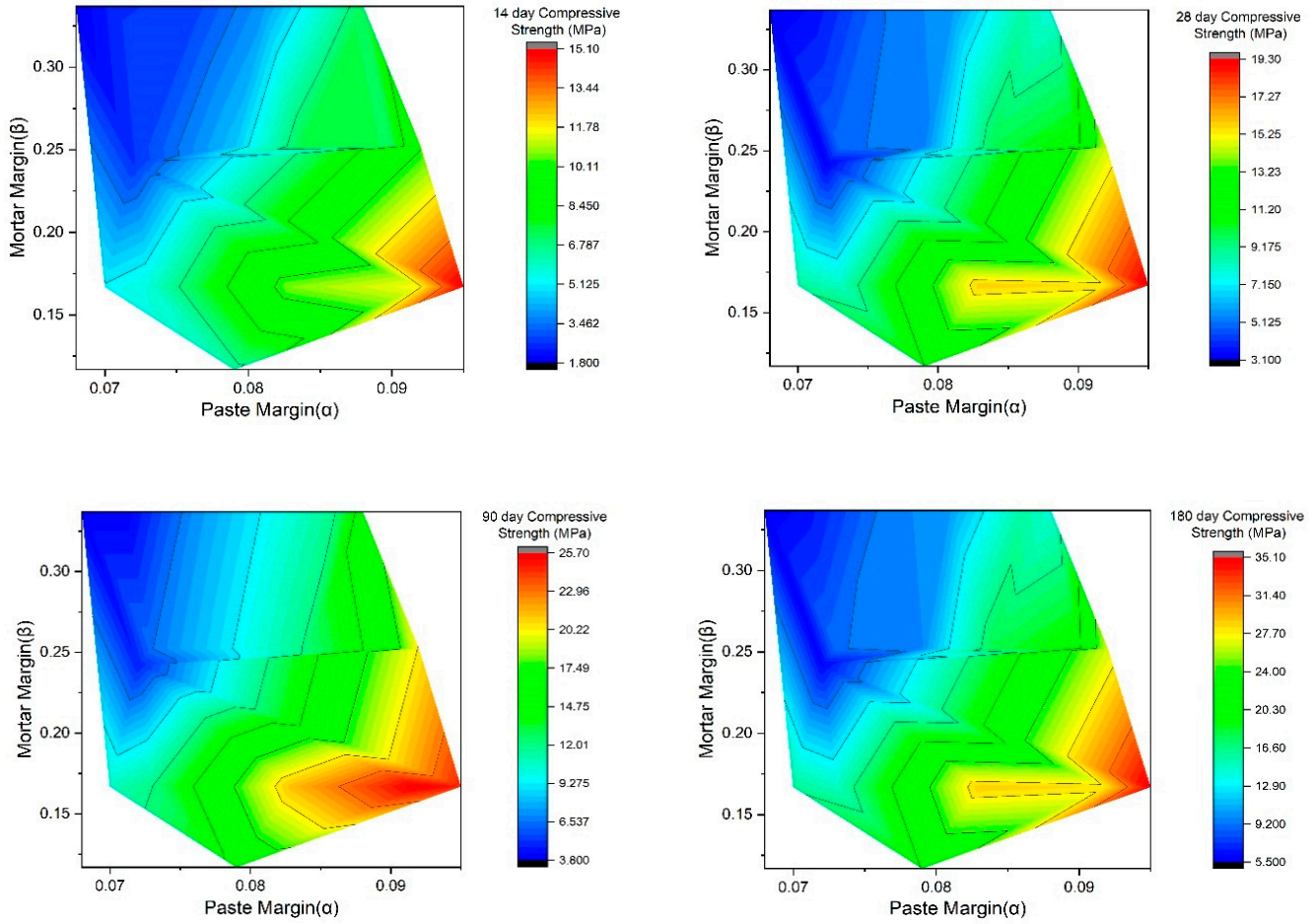

Figure 4. Relationship between paste and mortar margins and compressive strength development.

4.2. Discussion

4.2.1. Laboratory Test Samples of Lengshui Auxiliary CSGRD

The behaviour of the relationship between paste margin, mortar margin, and the compressive strength of CSGR (with the target being $C_{180}20$ compressive strength class) over several curing periods (7-day, 28-day, 90-day, and 180-day periods) has been studied. The Pearson correlation coefficients, t-statistics, and *p*-values were calculated to determine the strength and significance of these relationships between the paste margin, mortar margin, and compressive strength, as shown in Table 22. The discussion of the analysis for Lengshuihe Auxiliary CSGRD is provided below.

Table 22. Lengshuihe Auxiliary CSGRD.

Margins	Test Age (days)	Pearson Correlation (r)	t-Statistics	*p*-Value	Overall Remarks
Paste Margin (α)	07	0.172	0.741	4.67×10^{-1}	Weak-to-moderate positive correlation and no statistically significant relationships
	28	0.197	0.853	4.04×10^{-1}	
	90	0.221	0.784	4.43×10^{-1}	
	180	0.418	1.382	1.84×10^{-1}	
Mortar Margin (β)	07	−0.269	−1.185	2.51×10^{-1}	Weak-to-moderate negative correlation and no statistically significant relationships
	28	−0.216	−0.936	3.62×10^{-1}	
	90	−0.003	−0.011	9.91×10^{-1}	
	180	0.204	0.624	5.40×10^{-1}	

(i) Overview: Paste Margin vs. Compressive Strength Development

From Table 22, the Pearson correlation coefficients for paste margin and compressive strength revealed a generally weak positive relationship across all curing periods. Specifically, the correlation coefficients were 0.172, 0.197, 0.221, and 0.418 for the 7-day, 28-day, 90-day, and 180-day compressive strengths, respectively. The corresponding t-statistics (0.741, 0.853, 0.784, and 1.382) suggest that these correlations are not statistically significant as the condition of $p < 0.05$ was not satisfied. This indicates that, while there is a slight trend suggesting that an increase in paste margin might be associated with higher compressive strength over time, the relationship was weak and not strongly predictive.

As the curing period increases, the strength of the correlation does as well, reaching a moderate level by the 180-day mark. However, the overall statistical insignificance suggests that paste margin alone may not be a strong determinant of compressive strength, and other factors such as aggregate quality, sand ratio, fine content, water–cement ratio, curing condition, and age are likely to play a more critical role in influencing the CSGR performance over time [14–17].

The Pearson correlation coefficients and corresponding *p*-values for the paste margin and compressive strength across various test ages (7, 28, 90, and 180 days) show that the relationship between paste margin and compressive strength was generally weak.

(a) Insight into Paste Margin vs. Compressive Strength Development

The data in Table 22 provide insights into the relationship between paste margin and compressive strength at different curing ages: 7 days, 28 days, 90 days, and 180 days. The details are provided as follows:

- A 7-Day Test Age: The Pearson correlation coefficient is 0.172 with a *p*-value of 0.467. This suggests a very weak positive correlation between paste margin and compressive strength, which is not statistically significant.
- A 28-Day Test Age: The correlation slightly improves to 0.197 with a *p*-value of 0.404. Although the relationship strengthens slightly, it remains weak and statistically insignificant.
- A 90-Day Test Age: The coefficient increases to 0.221 with a *p*-value of 0.443, indicating a continued weak relationship, still not statistically significant.

- A 180-Day Test Age: The correlation coefficient jumps to 0.418 with a *p*-value of 0.184. While this shows a moderate positive correlation, the relationship is still not strong enough to be deemed statistically significant.

(b) Remarks on Paste Margin and Compressive Strength Development

The paste data suggest that the relationship between paste margin and compressive strength becomes moderately positive as the curing time increases [17]. However, none of the correlations are statistically significant, implying that the paste margin alone does not have a strong predictive power for compressive strength [14].

(ii) Overview: Mortar Margin vs. Compressive Strength Development

In contrast, the relationship between mortar margin and compressive strength fluctuated between weak negative and weak positive correlations across the curing periods, as indicated in Table 22. The Pearson coefficients were −0.269, −0.216, −0.003, and 0.204 for the 7-day, 28-day, 90-day, and 180-day compressive strengths, respectively. These results suggest that there is a slight inverse relationship between mortar margin and compressive strength at early stages, with higher mortar margins possibly leading to lower strength. However, by 180 days, this relationship becomes weakly positive, though still statistically insignificant based on the t-statistics (−1.185, −0.936, −0.011, and 0.624).

The lack of a strong, consistent relationship between mortar margin and compressive strength suggests that the mortar margin may not be the only critical factor in determining the compressive strength of CSGR, particularly as the material or prepared samples mature [14].

(a) Insight into Mortar Margin vs. Compressive Strength Development

For the mortar margin in Table 22, the Pearson correlation coefficients and *p*-values indicate a fluctuating relationship with compressive strength, ranging from weak negative to weak positive correlations across the various test ages. The details are provided as follows:

- A 7-Day Test Age: The Pearson correlation coefficient is −0.269 with a *p*-value of 0.251. This suggests a weak negative correlation, which is not statistically significant.
- A 28-Day Test Age: The correlation improves slightly to −0.216 with a *p*-value of 0.362, but it remains weak and statistically insignificant.
- A 90-Day Test Age: The correlation is nearly non-existent at −0.003 with a *p*-value of 0.991, indicating no meaningful relationship between mortar margin and compressive strength.
- A 180-Day Test Age: The relationship turns positive with a Pearson coefficient of 0.204 and a *p*-value of 0.540. This indicates a weak positive correlation, though it is also not statistically significant.

(b) Remarks on Mortar Margin and Compressive Strength Development

The mortar data in Table 22 reveal that the relationship between mortar margin and compressive strength is inconsistent and weak. None of the correlations are statistically significant, suggesting that the mortar margin is not a reliable predictor of compressive strength in this dataset.

(iii) Overall Remarks on both Paste and Mortar Margins and Compressive Strength Development

From Table 22, both the paste and mortar margins in the mix proportioning of the materials showed weak correlations with compressive strength across the various test ages. As curing time increases, the relationship for paste margin tends to strengthen slightly, but neither paste nor mortar margins demonstrated statistically significant relationships with compressive strength. This suggests that while these margins may influence CSGR properties, their impact on compressive strength development was likely overshadowed by other variables beyond paste and mortar margins that could have affected

hydration product formation, leading to weak bonds between constituents based on the compression test data analysis [4], such as the aggregate type, type of cement, and fly as well as their properties, water–cement ratio, and curing conditions (refer to SL678-2014, the technical guidelines for cemented granular materials for the requirement for aggregates, sand ratio, apparent density, binders, and water/binder ratio) [14]. Also, the outcome related well to the USACE experiment findings on the HCRCC mixes test, which explained the effect of too much Stone Powder (SP) on workability and compressive strength. The fine aggregate in this experiment was found to have a high fine content, which increased the demand for water during mixing, adversely affecting workability and strength development negatively over time [16,17].

4.2.2. Laboratory Test Samples of Shaping I Hydropower CSGRD

The relationship between paste margin, mortar margin, and the compressive strength of CSGR (with the target being $C_{180}20$ compressive strength class) over several curing periods (14-day, 28-day, 90-day, and 180-day periods) has been studied. The Pearson correlation coefficients, t-statistics, and *p*-values were calculated to determine the strength and significance of these relationships between the paste margin, mortar margin, and compressive strength, as indicated in Table 23. The discussion of the results for the Shaping I CSGRD is provided below:

Table 23. Shaping I Hydropower CSGRD.

Margins	Test Age (days)	Pearson Correlation (r)	t-Statistics	*p*-Value	Overall Remarks
Paste Margin (α)	14	0.844	6.785	1.07×10^{-5}	Strong positive correlation and statistically significant relationships
	28	0.787	5.252	1.06×10^{-4}	
	90	0.850	6.986	7.96×10^{-6}	
	180	0.787	5.252	1.06×10^{-4}	
Mortar Margin (β)	14	−0.544	2.568	1.96×10^{-2}	Moderate-to-strong negative correlation and statistically significant relationships
	28	−0.628	3.222	5.3×10^{-3}	
	90	−0.565	2.748	1.46×10^{-2}	
	180	−0.628	3.222	5.30×10^{-3}	

(i) Paste Margin vs. Compressive Strength Development

These values in Table 23 suggest a strong positive relationship between paste margin and compressive strength, with the strength of the correlation increasing as the curing period extends. The correlation coefficients for 14-day, 28-day, 90-day, and 180-day curing periods were 0.844, 0.787, 0.850, and 0.787. The corresponding t-statistics (6.785, 5.252, 6.986, and 5.252) and *p*-values (1.07×10^{-5}, 1.06×10^{-4}, 7.96×10^{-6}, and 1.06×10^{-4}) further confirm that these correlations are statistically significant across all periods, indicating that an increase in paste margin is consistently associated with higher compressive strength. This strong and statistically significant correlation implies that paste margin was a critical factor in determining the compressive strength of CSGR in this dataset. The increasing correlation over time also suggests that the influence of paste margin becomes more pronounced as the CSGR cures, making it an important variable in the long-term development of CSGR strength.

(a) Insight into Paste Margin vs. Compressive Strength Development

The data in Table 23 provide insights into the relationship between paste margin and compressive strength at different curing ages: 14 days, 28 days, 90 days, and 180 days. The details are provided as follows:

- A 14-Day Test Age: The Pearson correlation coefficient is 0.844 with a *p*-value of 1.07×10^{-5}. This strong positive correlation suggests a significant relationship between paste margin and compressive strength at the early curing stage. The

very low *p*-value indicates that this result is statistically significant, affirming the positive influence of paste margin on the early strength of the CSGR.

- A 28-Day Test Age: The correlation decreases slightly to 0.787 with a *p*-value of 1.06×10^{-4}. While the relationship remains strong and statistically significant, the slight decrease in the correlation coefficient suggests that other factors may begin to influence compressive strength as the curing process continues.
- A 90-Day Test Age: The correlation coefficient increases slightly to 0.850 with a *p*-value of 7.96×10^{-6}. This again indicates a strong positive relationship, reaffirming the significant impact of paste margin on compressive strength as the CSGR continues to mature.
- A 180-Day Test Age: The correlation returns to 0.787 with a *p*-value of 1.06×10^{-4}, mirroring the results seen at 28 days. This consistency in correlation strength between the 28-day and 180-day marks suggests a stabilized relationship between paste margin and long-term compressive strength.

(b) Remarks on Paste Margin and Compressive Strength Development

The strong positive correlations across all curing periods in Table 23, coupled with highly significant *p*-values, indicate that paste margin is a critical factor in determining compressive strength [14]. The data suggest that increasing paste margin consistently contributes to higher compressive strength, especially in the early stages, with this effect being sustained as the CSGR matures.

(ii) Mortar Margin vs. Compressive Strength Development

These negative coefficients (−0.544, −0.628, −0.565, −0.628 for 7-day, 28-day, 90-day, and 180-day curing periods) shown in Table 23 indicate an inverse relationship between mortar margin and compressive strength, where an increase in mortar margin is associated with a decrease in compressive strength. The strength of this negative correlation, however, is moderate and decreases slightly over time, suggesting that while the mortar margin does have an impact on compressive strength, its influence diminishes as the CSGR cures. The t-statistics (2.568, 3.222, 2.748, and 3.222) and the *p*-values (1.96×10^{-2}, 5.3×10^{-3}, 1.46×10^{-2}, and 5.3×10^{-3}) for these correlations indicate that while the relationship is statistically significant, it is weaker compared to the paste margin's influence. This suggests that although mortar margin negatively affects compressive strength, its impact is less critical, especially as the CSGR matures [4,17].

(a) Insight into Mortar Margin vs. Compressive Strength Development

From Table 23, the relationship between mortar margin and compressive strength is inverse, as indicated by the negative Pearson correlation coefficients at all curing ages. The details are provided as follows:

- 14 Days: The Pearson correlation coefficient is −0.544, with a *p*-value of 1.96×10^{-2}. This moderate negative correlation indicates that a higher mortar margin is associated with lower compressive strength at this early stage, and the statistically significant *p*-value suggests that this relationship is reliable.
- 28 Days: The correlation strengthens to −0.628, with a *p*-value of 5.3×10^{-3}, implying a more pronounced negative impact of mortar margin on compressive strength as the CSGR continues to cure. The stronger correlation and lower *p*-value emphasize the significance of this negative relationship.
- 90 Days: The correlation weakens slightly to −0.565, with a *p*-value of 1.46×10^{-2}. Although the negative relationship persists, the slight reduction in correlation strength may indicate that other factors begin to mitigate the impact of mortar margin on compressive strength.
- 180 Days: The correlation returns to −0.628, with a *p*-value of 5.3×10^{-3}, similar to the 28-day data. This suggests that the negative impact of mortar margin on compressive strength is sustained over time.

(b) Remarks on Mortar Margin and Compressive Strength Development

The consistent negative correlations and significant *p*-values across all curing periods in Table 23 suggest that mortar margin detrimentally affects compressive strength [4]. This effect is particularly strong at 28 days and is sustained through to 180 days. The data imply that a higher mortar margin could lead to weaker CSGR, and controlling this factor is crucial for achieving desired strength outcomes [14]. Existing research works suggested that the sand ratio should be modified to improve the workability margin in such cases [15,16]. SL 678-14 also recommends a sand ratio between 18 and 35% [14].

(iii) Overall Remarks on both Paste and Mortar Margins and Compressive Strength Development

From Table 23, the analysis of paste and mortar margins reveals critical insights into their roles in CSGR performance. The paste margin consistently shows a positive correlation with compressive strength development, highlighting its importance in achieving higher strength, especially as the CSGR cures. Conversely, the mortar margin exhibits a negative correlation, which relates well with the findings of USACE on HCRCC , suggesting that higher mortar content may weaken the CSGR, particularly in the long term, and therefore there was the need to regulate and control the sand ratio and fine content to achieve the design requirement of the project [16,17].

5. Conclusions

Based on the analysis of the paste and mortar margins of test samples for the Rich-Mix CSGR material, the following conclusions can be drawn:

1. The optimum range of paste and mortar margins (α and β) are 1.05~1.09 and 1.15~1.25, respectively, fill the voids in the fine and coarse aggregates with a surplus for workability margin, providing better enhancement of compressive strength development in CSGRD projects when the rich-mix $C_{180}20$ strength class of CSGR for aggregates of apparent density ≥2450 kg/m^3 needs to be achieved reliably, quickly, and economically.
2. The significance of the paste margin on the compressive strength development implies that paste margin is a critical factor in determining the compressive strength of rich-mix CSGR; therefore, cementitious content ≥80 kg/m^3 (cement ≥ 40 kg/m^3) and water/binder should range from 0.7~ 1.3 need to be considered for parent CSGR, cement slurry of 8%~12% addition rate and w/c of 0.5~0.6 for rich mix preparation.
3. The consistent negative correlations and significant p-values across nearly all curing periods suggest that an uncontrollable mortar margin has a detrimental effect on the compressive strength development of CSGR, which is powerful at 28 days and persists through 180 days. The data imply that a higher mortar margin could lead to weaker CSGR, making controlling the sand ratio between 18% and 35% crucial.
4. The α and β values approached their optimum as the VC value decreased significantly, enhancing workability. Notably, a VC value of 2 to 8 s was associated with rapid and high compressive strength development towards the $C_{180}20$ strength class and warrants further study and application in future projects.
5. The aggregate type, fine content, type of cementitious materials, type and extent of curing, and others play vital roles in the compressive strength development of CSGR, in addition to the critical roles of paste and mortar margins. Researchers must refer to the technical guidelines for cemented granular materials (SL678-2014) [14].

Further studies on the effects of mud content, fine content, admixture content, and sand ratio are ongoing to analyze and understand how material properties impact the performance of CSGR, specifically on Rich-Mix and Grout-Enriched Vibrated CSGR in CSGRD applications, aiming to establish criteria for performance enhancement.

Author Contributions: Formal analysis and investigation, Y.W. (Yangfeng Wu) and W.A.B.; methodology, W.A.B.; resources, B.J.; writing—original draft, W.A.B.; writing—review and editing,

W.A.B., J.J., and Y.W. (Yue Wang); supervision, J.J., C.Z., and Y.W. (Yue Wang); funding acquisition, J.J. All authors have read and agreed to the published version of the manuscript.

Funding: This research is financially supported by the National Key Research and Development Plan of China under Grant No. 2018 YFC0406801.

Institutional Review Board Statement:

Informed Consent Statement:

Data Availability Statement: All relevant data are included in the paper.

Acknowledgments: This study was supported by the State Key Laboratory of Simulation and Regulation of Water Cycles in River Basins.

Conflicts of Interest: The authors declare no conflicts of interest.

Abbreviations

The following abbreviations are used in the manuscript

CSGR	Cemented Sand, Gravel, and Rock
CSGRD	Cemented Sand, Gravel, and Rock Dam
CMD	Cemented Material Dam
α	Paste Margin Value
β	Mortar Margin Value
$C_{180}20$	Rich-Mix (High-Cementitious) CSGR with Compressive Strength of 20 MPa at 180 days
SL678-2014	Technical Guideline for Cemented Granular Materials issued by the Ministry of Water Resources of China in 2014
VC	Vibrating–Compacted Value
CSG	Cemented Sand and Gravel
RCC	Roller Compacted Concrete
HCRCC	High-Cementitious Roller Compacted Concrete
SHCRCC	Super-High-Cementitious Roller Compacted Concrete
MSA	Maximum Size of Aggregate
CVC	Conventional Vibrated Concrete
ICOLD	International Committee on Large Dams
USACE	United States Army Corps of Engineers
USBR	United States Bureau of Reclamation

Appendix A

- **Case Study Project 1: Lengshuihe Auxiliary CSGRD Project**

The Lengshui River Reservoir, located in Mugou Town, Shuicheng County, Guizhou Province, is part of the Wu River system in the Yangtze River Basin. It has a catchment area of 36.5 km^2 (11.8 km^2 clear flow, 9.8 km^2 subsurface flow, 14.9 km^2 depression) and a main river channel 7.54 km long with an average gradient of 61.5%. The reservoir's annual average inflow is 17.62 million m^3, with a rate of 0.559 m^3/s. Its normal water level is 1767 m, holding 8.52 million m^3, and the dead water level is 1737 m, with a dead storage of 1.2 million m^3. The check flood level is 1769.6 m, and the total storage is 9.56 million m^3. It is a small (Type 1) project, Grade IV. The reservoir supplies 9.31 million m^3 of water to five towns, 720,000 m^3 for irrigation (80% assurance), and releases 1.84 million m^3 for the environment, irrigating 1,764,000 m^2 of farmland (312,667 m^2 of paddy fields and 1,451,333 m^2 of dry land).

The auxiliary dam, as shown in Figure A1, 60 m inside the reservoir from the saddle point, is 115 m long with an azimuth of N3.307°E, a crest at 1771.5 m, a maximum height of 39.5 m, and a width of 6 m. The upstream slope is 1:0.3, and the downstream slope is 1:0.75. Three dam types were considered: clay core wall, concrete-faced rockfill and cemented sand, gravel, and rock (CSGR). The CSGRD, chosen for its moderate cost, ease of

construction, and environmental benefits, was built using $C_{180}6$ for the body of the dam and Rich-Mix ($C_{180}20$) for seepage control and cushion layers. CSGR with a volume of about 40,000 m^3 was used for body construction. Construction started in August 2022 and finished in December 2022.

Figure A1. During the construction of Lengshuihe Auxiliary CSGRD.

- **Case Study Project 2: Shaping I Hydropower CSGRD Project**

Located on the mainstream of the Dadu River in Jinkouhe District, Leshan City, Sichuan Province, this concrete and CSGR mixed dam has a maximum height of 63 m, a dam crest elevation of 581.00 m, and a total dam crest length of 327 m. It is the world's first large-scale hydropower project to use CSGRD for its main structure. The total volume of cemented sand, gravel, and rock is approximately 650,000 m^3. The application of cemented materials dam technology (CMD) demonstrates advantages in economy, speed, safety, and environmental protection. The project has achieved a record of filling 100,000 m^3 per month using two sets of mixing equipment.

The total storage capacity of the power station is 21.23 million m^3, with a normal water storage level of 577.00 m and a corresponding storage capacity of 18.67 million m^3. The regulating storage capacity is 4.91 million m^3, allowing for daily regulation. The power station has a total installed capacity of 360 MW and operates jointly with Shuangjiangkou and Pugou to guarantee an output of 119 MW and a multi-year average power generation of 1.635 billion kWh. The power supply is provided to the Sichuan Power Grid. $C_{180}20$ CSGR material shall be used to construct cushion layers, protection, and seepage control layers within some sections of the body of the dam. The project began in 2023 and is currently under construction, as shown in Figure A2.

(**a**) (**b**)

Figure A2. (**a**) CSGR continuous mixer set-up. (**b**) Dam site preparations.

- **Governing Equations for Paste and Alpha Margins**

$$\alpha = P_{tv} - FA_{sv} \times \left(\frac{FA_{vv}}{FA_{sv}}\right) \quad \text{(A1)}$$

where α is the paste margin; P_{tv} is the total paste volume per unit of volume; FA_{sv} is the total volume of fine aggregate per unit of volume; FA_{vv} is the total void volume of the fine aggregate per unit of volume; and the ratio $\frac{FA_{vv}}{FA_{sv}}$ is the void ratio of the fine aggregate.

$$\beta = P_{tv} + FA_{tv} - CA_{sv} \times \left(\frac{CA_{vv}}{CA_{sv}}\right) \quad \text{(A2)}$$

where β is the mortar margin; FA_{tv} is the total volume of fine aggregate per unit of volume; CA_{sv} is the total volume of coarse aggregate per unit of volume; CA_{vv} is the total void volume of the coarse aggregate per unit of volume; and the ratio $\frac{CA_{vv}}{CA_{sv}}$ is the void ratio of the coarse aggregate. The total volume of the mix is given by the following expression:

$$T_v = V_{agg} + V_{paste} \quad \text{(A3)}$$

where T_v is the total volume; V_{agg} (fine aggregate and coarse aggregate) is the volume of aggregates; and V_{paste} (cement, fly ash, water, and admixtures) is the volume of paste. The solid volume of aggregates and pastes is computed from the following equation:

$$\Phi = \frac{P_{b\,m}}{SG_m \, xP_w} \times F_m \ (\%) \quad \text{(A4)}$$

where Φ is the packing density or volume of solid material; $P_{b\,m}$ is the bulk density of material [30]; SG_m is the specific gravity of material; P_w is the density of water; and F_m is the fraction of material in the total volume of the mix [22].
The void volume can be computed as follows:

$$V_v = T_{vs} - \phi \quad \text{(A5)}$$

where V_v is the void volume within the solid content, and T_{vs} is the total volume of the solid content. The void volume, or the void ratio, is influenced by the aggregate grading and the ability to consolidate and compact the fresh mixture [22]

- **Sample Calculation of the Determination of the Pearson coefficient and Statistical significance**

Computations of the Pearson correlation and the statistical significance of the paste and mortar margins with the 14th-day test age compressive strength of the Shaping I Hydropower CSGRD are provided as follows:

(i) Data on the α, β, and the 14th-day compressive strength values were collected as indicated in Table 15.

(ii) Verification of criteria for the usage of the Pearson correlation coefficient:

  (a) The paste margin (0.068, 0.072, 0.070, …, 0.095) is continuous.
  (b) The mortar margin (0.337, 0.242, …, 0.167) is continuous.
  (c) The 14th-day compressive strength (MPa) (1.8, 2.6, 5.2, …, 15.1) is continuous. This criterion is met, as the variables are continuous by observation. The values can change smoothly and are not confined to specific points, allowing for a wide range of possibilities.
  (d) Checking the linearity of the relationship between the variables. The linearity of the paste and mortar margins with the 14th-day compressive strength was assessed visually using a scatter plot or statistical linear regression in Figure A3 (only the paste margin and the same applies to the mortar margin). To check linearity, Y, the dependent variable (14th-day compression strength), was plotted against X, the independent variable (paste or mortar margin), to see if the points roughly followed a straight line, and then the linear regression model was

fitted, and the fit was inspected visually as shown in Figure A3. From the scatter plot in Figure A3, the parameters are linear.

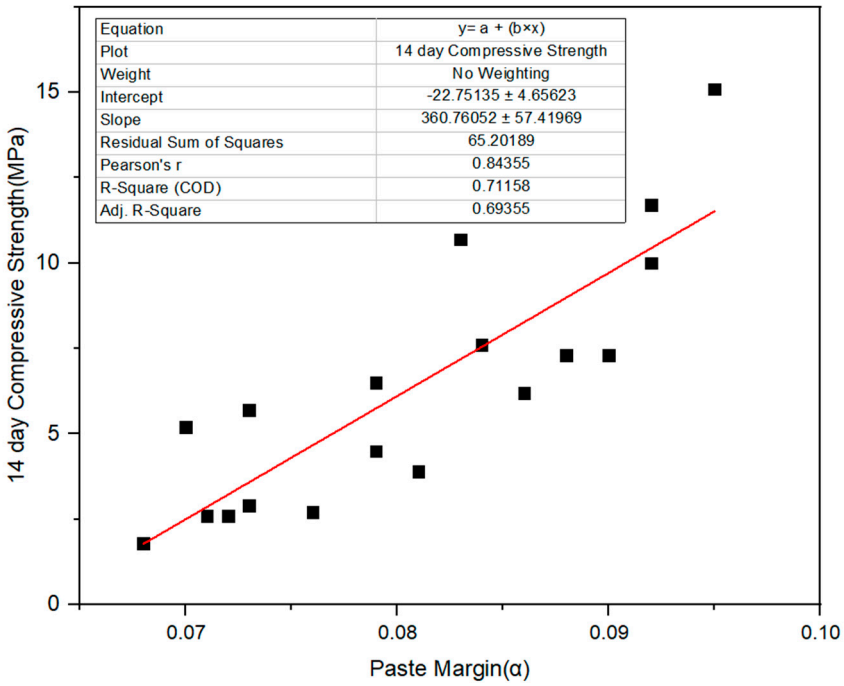

Figure A3. α vs. 14th-day compressive strength.

(e) Checking how closely the data are normally distributed.

Due to the complexity of the Shapiro–Wilk expression initially proposed, the *p*-values were computed using Python's scipy.stats.shapiro() function version v1.14.1, which automated the calculation. The Shapiro–Wilk test *p*-values were obtained using a computational approach built into the statistical software, which handled the complexities of the calculation. The *p*-values were derived for each dataset using the steps below:

(i) Input data: The data for paste margin, mortar margin, and 14th-day compression strength were entered into the function.
(ii) Execution of Shapiro–Wilk test: The scipy.stats.shapiro() function was applied to each dataset. This function internally computed the test statistic W and then determined the *p*-value associated with that W based on the sample size and distribution.
(iii) Output of the *p*-value: The function returned both the W statistic and the *p*-value, which assessed the data normality.
(iv) Results from the Python code:
- Paste margin *p*-value: $p = 0.364$.
- Mortar margin *p*-value: $p = 0.0589$.
- 14th-day compression strength *p*-value: $p = 0.162$.

(v) These *p*-values indicate whether the data follow a normal distribution.
- Paste margin: $p > 0.05$, approximately normal.
- Mortar margin: $p > 0.05$, approximately normal.
- 14th-day compression strength: $p > 0.05$, approximately normal.

(vi) Conclusion: The paste and mortar margins and 14th-day compression strength data meet the normality assumption.

(f) Homoscedasticity: The Variability of One Variable Should Be Similar Across All Values of the Other Variable

Based on the principles of the Breusch–Pagan test, the *p*-value from the test (paste and mortar margins and the 14th-day compressive strength) was greater than 0.05, which suggested that there is no evidence to reject the null hypothesis of homoscedasticity, meaning that the variance of the residuals is constant, and the data meet the assumption of homoscedasticity.

(iii) Calculation of the Pearson correlation coefficient and statistical significance using the paste margin and the 14th-day compressive strength test.

The calculation for paste margin and compression strength at 14 days is as follows:

- Calculation of the mean, derived from Table 20:

$$\ddot{x}_{paste} = \frac{1}{18}\sum_{i=1}^{18} x_i = \frac{0.068 + 0.072 + \cdots + 0.095}{18} = 0.0777$$

$$\ddot{y}_{14d} = \frac{1}{18}\sum_{i=1}^{18} \ddot{y}_i = \frac{1.8 + 2.6 + \cdots + 15.1}{18} = 6.3833$$

- Calculation of the Pearson correlation:

$$r_{14d} = \frac{\Sigma(x_i - \ddot{x}_{paste})(y_i - \ddot{y}_{14d})}{\sqrt{\Sigma(x_i - \ddot{x}_{paste})^2 \Sigma(y_i - \ddot{y}_{14d})^2}} = \frac{0.025}{\sqrt{0.00195 x 419.57}} = 0.843$$

- Calculation of the t-statistic:

$$t = \frac{r_{test\ age}\sqrt{n_{number\ of\ samples\ in\ column} - 2}}{\sqrt{1 - r_{test\ age}{}^2}} = \frac{0.843 x \sqrt{18-2}}{0.538} = 6.27$$

- Determination of the *p*-value:

The *p*-value corresponding to the t-statistic of 6.27 with (18−2) = 16 degrees of freedom is approximately 1.07×10^{-5} from statistical tables. This extremely small *p*-value indicates that the correlation between the paste margin and compression strength at 14 days is statistically significant.

(iv) Calculation of the Pearson correlation coefficient and statistical significance using the mortar margin and the 14th-day compressive strength test. The calculation for mortar margin and compression strength at 14 days is as follows:

- Calculation of the mean from Table 20:

$$\ddot{x}_{mortar} = \frac{1}{18}\sum_{i=1}^{18} x_i = \frac{0.337 + 0.242 + \cdots + 0.167}{18} = 0.2496$$

$$\ddot{y}_{14d} = \frac{1}{18}\sum_{i=1}^{18} \ddot{y}_i = \frac{114.9}{18} = 6.3833$$

- Calculation of the Pearson coefficient:

$$r_{14d} = \frac{\Sigma(x_i - \ddot{x}_{mortar})(y_i - \ddot{y}_{14d})}{\sqrt{\Sigma(x_i - \ddot{x}_{mortar})^2 \Sigma(y_i - \ddot{y}_{14d})^2}} = \frac{-7.69}{\sqrt{0.2484 x 419.57}} = -0.544$$

- Calculation of the t-statistic:

$$t = \frac{r_{test\ age}\sqrt{n_{number\ of\ samples\ in\ column} - 2}}{\sqrt{1 - r_{test\ age}{}^2}} = \frac{-0.544 x \sqrt{18-2}}{0.839} = -2.59$$

- Determination of the *p*-value:

The *p*-value corresponding to the t-statistic of −2.59 with (18−2) = 16 degrees of freedom is approximately 1.96×10^{-2} from statistical tables. This extremely small *p*-value indicates that the correlation between the mortar margin and compression strength at 14 days is statistically significant.

(v) Remarks: The above steps are the same for the other curing periods in both projects (7, 28, 90, and 180 days) and for both paste and mortar margins.

Appendix B

Figure A4. In situ aggregate sampling and gradation analysis.

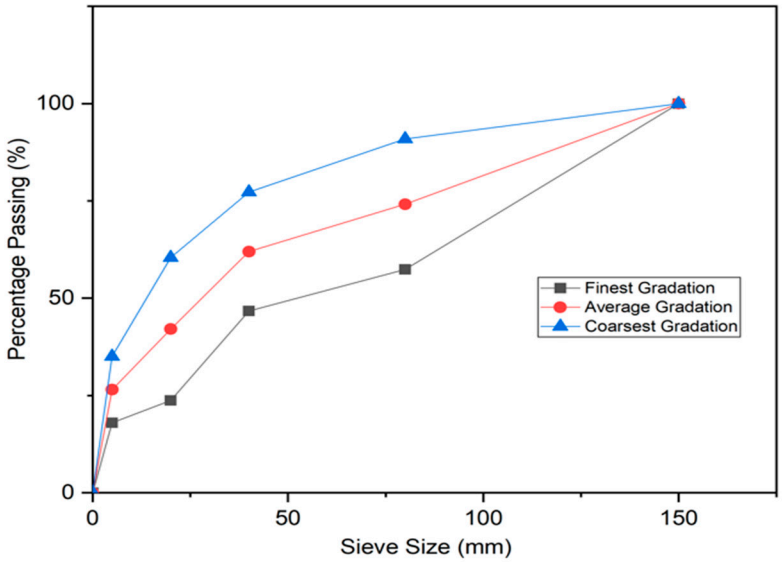

Figure A5. Aggregate gradation envelope showing the finest, average, and coarsest gradations.

Figure A6. Workability test (VC test) using the Vebe apparatus.

References

1. Jia, J.; Lino, M.; Jin, F.; Zheng, C. The Cemented Material Dam : A New, Environmentally Friendly Type of Dam. *Engineering* **2016**, *2*, 490–497.
2. Jia, J.; Wang, S.; Zheng, C.; Chen, Z.; Wang, Y. FOSM-based shear reliability analysis of CSGR dams using strength theory. *Comput. Geotech.* **2018**, *97*, 52–61. https://doi.org/10.1016/j.compgeo.2018.01.003.
3. Zhongwei, L.; JinSheng, J.; Wei, F.; FengLing, M.; Cuiying, Z. Shear Strength of Cemented Sand Gravel and Rock Materials. *Sains Malays.* **2017**, *46*, 2101–2108.
4. Jia, J.; Baah, W.A.; Zheng, C.; Ding, L.; Wu, Y. New stress-strain model and intelligent quality control technology for cemented material dam. *J. Intell. Constr.* **2023**, *2*, 9180033. https://doi.org/10.26599/jic.2023.9180033.
5. Wu, Y.; Jia, J.; Zheng, C.; Jia, B.; Wang, Y.; Baah, W.A. A New Method for Constructing the Protection and Seepage Control Layer for CSGR Dam and Its Application. *Appl. Sci.* **2024**, *14*, 5423.
6. Yuan, P.; He, Y.; Wang, Y. Study on seismic safety of Poshitougou flood intercepting dam. *IOP Conf. Ser. Earth Environ. Sci.* 2021, 861, 072073. https://doi.org/10.1088/1755-1315/861/7/072073.
7. Chen, J.; Liu, P.; Xu, Q.; Li, J. Seismic analysis of hardfill dams considering spatial variability of material parameters. *Eng. Struct.* **2020**, *211*, 110439. https://doi.org/10.1016/j.engstruct.2020.110439.
8. Guo, L.; Zhang, J.; Guo, L.; Wang, J.; Shen, W. Case Studies in Construction Materials Research on profile design criteria of 100 m CSG dams. *Case Stud. Constr. Mater.* **2022**, *16*, e01137. https://doi.org/10.1016/j.cscm.2022.e01137.
9. Cai, X.; Zhang, Y.; Guo, X.; Zhang, X.; Li, F.; Zhang, T. Review on research progress of cemented sand and gravel dam. *Sci. Eng. Compos. Mater.* **2022**, *29*, 438–451.
10. Ayagh, A.G.; Mohammadian, A. Optimum characteristic compressive strength for cmds (case study: Dasht-e-palang dam). *Long Term Behav. Environ. Friendly Rehabil. Technol. Dams* **2017**, 243–250. https://doi.org/10.3217/978-3-85125-564-5-036.
11. Yoshimura, S.; Takasugi, S. Construction of Apporo Trapezoidal CSG Dam. In *Innovative Technologies for Dams and Reservoirs toward the Future Generations*; ICOLD: Chatou, France, 2012; pp. 13–18.
12. Jia, J.; Zheng, C.; Li, S.; Ding, L.; Wu, Y. Optimising structural function designing and new practices of cemented material dams in China. *Hydropower Dams* **2020**, 1–6.
13. Jia, J.; Liu, Z.; Feng, W.; Ma, F.; Zheng, C.; Wang, Y. Water Pressure Induced Corrosion of Cemented Sand, Gravel, and Rock (CSGR). *Arab. J. Sci. Eng.* **2018**, *43*, 2083–2092. https://doi.org/10.1007/s13369-017-2698-5.
14. *SL678-2014*; Technical Guideline for Cemented Material Dams. China Water & Power Press: Beijing, China, 2014.
15. Mahmoodi, K.; Noorzad, A.; Mahboubi, A.; Alembagheri, M. Seismic performance assessment of a cemented material dam using incremental dynamic analysis. *Structures* **2021**, *29*, 1187–1198. https://doi.org/10.1016/j.istruc.2020.12.015.
16. Feng, W.; Jia, J.; Liu, Z.; Wang, Y. Study on quantification method for aggregate gradation of discrete Cemented Sand Gravel and Rock. *IOP Conf. Ser. Earth Environ. Sci.* **2019**, *330*, 042031. https://doi.org/10.1088/1755-1315/330/4/042031.
17. Aosaka, Y.; Tsutsui, S.; Miki, T. Study on Mix Proportion Design Procedure for Super-high Cementitious RCC with Stone Powder Replacement. *J. Adv. Concr. Technol.* **2023**, *21*, 123–135. https://doi.org/10.3151/jact.21.123.
18. Ashtankar, V.B.; Chore, H.S. Development of design mix roller compacted concrete dam at Middle Vaitarana. *Adv. Concr. Constr.* **2014**, *2*, 125–144. https://doi.org/10.12989/acc.2014.2.2.125.
19. Chonggang, S. Roller compacted concrete dams in China. *Int. Water Power Dam Constr.* **1991**, *43*, 45–49.
20. Chen, S.H. *Hydraulic Structures*; Springer: Berlin/Heidelberg, Germany, 2015. https://doi.org/10.1007/978-3-662-47331-3.
21. Rath, B.; Deo, S.; Ramtekkar, G. A Proposed Mix Design of Concrete with Supplementary Cementitious Materials by Packing Density Method. *Iran. J. Sci. Technol. Trans. Civ. Eng.* **2020**, *44*, 615–629. https://doi.org/10.1007/s40996-020-00362-4.
22. Mohammed, M.H.; Pusch, R.; Al-Ansari, N.; Knutsson, S. Optimization of Concrete by Minimizing Void Volume in Aggregate Mixture System. *J. Adv. Sci. Eng. Res.* **2012**, *2*, 208–222.
23. Zhao, X.; He, Y. The permeable character of CSG Dams and their seepage fields. *Complexity* **2018**. https://doi.org/10.1155/2018/6498458.
24. *ASTM C 33/C33M*; Standard Specification for Concrete Aggregates. ASTM: West Conshohocken, PA, USA, 2023.
25. *ACI 211.1*; Standard Practice for Selecting Proportions for Normal, Heavyweight, and Mass Concrete (ACI 211.1-22). ACI: Detroit, MI, USA, 2022.
26. *ASTM C150/C150M*; Standard Specification for Portland Cement. ASTM: West Conshohocken, PA, USA, 2022. https://doi.org/10.1520/C0150.
27. *ASTM C618*; Standard Specification for Coal Fly Ash and Raw or Calcined Natural Pozzolan for Use in Concrete. ASTM: West Conshohocken, PA, USA, 2019. https://doi.org/10.1520/C0618-17A.10.1520/C0618-19.2.
28. *ASTM C1170*; Standard Test Method for Determining Consistency and Density of Roller-Compacted Concrete Using a Vibrating Table. ASTM: West Conshohocken, PA, USA, 2016. Available online: www.astm.org (accessed on 20 August 2024).
29. *ASTM C39/C39M*; Standard Test Method for Compressive Strength of Cylindrical Concrete Specimens. ASTM: West Conshohocken, PA, USA, 2021.
30. *C29/C29M*; Standard Test Method for Bulk Density ('Unit Weight') and Voids in Aggregate. ASTM: West Conshohocken, PA, USA, 2023.
31. *Chinese Standards SL/T 352-2020*; Test Code for Hydraulic Concrete SL/T 352. China Water & Power Press: Beijing, China, 2020. (In Chinese)

32. Sreedevi, S. Study of test for significance of Pearson's correlation coefficient. *Peer Rev. Ref. J.* **2022**, *816*, 11. Available online: http://ijmer.in.doi./2022/11.02.15 (accessed on 15 July 2024).
33. Chatterjee, S. A New Coefficient of Correlation. *J. Am. Stat. Assoc.* **2021**, *116*, 2009–2022. https://doi.org/10.1080/01621459.2020.1758115.
34. Li, Z.; Lu, D.; Gao, X. Analysis of correlation between hydration heat release and compressive strength for blended cement pastes. *Constr. Build. Mater.* **2020**, *260*, 1204–1236. https://doi.org/10.1016/j.conbuildmat.2020.120436.